Relating neuromuscular control to functional anatomy of limb muscles in extant archosaurs

Andrew R. Cuff[1], Monica A. Daley[1], Krijn B. Michel[1], Vivian R. Allen[1], Luis Pardon Lamas[1,2], Chiara Adami[3], Paolo Monticelli[3], Ludo Pelligand[3], John R. Hutchinson[1]

[1] Structure and Motion Laboratory, Department of Comparative Biomedical Sciences, Royal Veterinary College, Hawkshead Lane, North Mymms, Hertfordshire, AL9 7TA, United Kingdom.

[2] Current address: Faculdade de Medicina Veterinária, Universidade de Lisboa, Pólo 7, Universitário da Ajuda, 1300-477, Lisboa, Portugal.

[3] Queen Mother Hospital, Department of Clinical Science and Services, Royal Veterinary College, Hawkshead Lane, North Mymms, Hertfordshire, AL9 7TA, United Kingdom.

Abstract

Electromyography (EMG) is regularly used to help understand muscle activity patterns in animals. Seldom has it been used to compare across a range of species within a clade. Here we carry out a broad comparison of muscle activity patterns across a range of living archosaurs, with a primary focus on birds and hindlimbs. Fine wire EMG electrodes were implanted into the appendicular muscles of turkeys, pheasants, quail, guineafowl and tinamous as well as Nile crocodiles. The animals walked and ran at a range of speeds both overground and on treadmills during recordings of muscle electrical activity. Functionally similar muscles such as the lateral gastrocnemius exhibited similar EMG patterns at similar relative speeds across all birds. In the crocodiles, the EMG signals closely matched previously published data for alligators. The timing of lateral gastrocnemius activation was relatively later in crocodiles compared to birds, occurring only in stance phase; whereas in birds it begins late in swing phase. This difference may relate to the coordinated knee extension and ankle plantarflexion timing across the swing-stance transition in Crocodylia, unlike in birds where there is knee flexion and ankle dorsiflexion across swing-stance. No significant effects were found across the species for ontogeny, or between treadmill and overground locomotion. These data have value for understanding neuromuscular and functional diversity in archosaurian locomotor musculature as well as broader questions about conservatism vs. divergence in muscle function among vertebrates, which we address here.

Introduction

Animals move using coordinated patterns of muscular activity stimulated by motor neurons. The patterns of muscle activations are challenging to measure (1), but the electrical signals associated with neuromuscular excitation and thence activation can be obtained using electromyography (EMG). Integrating EMG with kinematic data and anatomical information can facilitate interpretation of the individual function of muscles (e.g. 1), particularly for muscles that have a similar morphology. For example, M. iliotibialis lateralis in birds has two heads covering most of the lateral aspect of the thigh: M. iliotibialis laterals pars preacetabulum (ILPR) and M. iliotibialis lateralis pars postacetabularis (ILPO), which originate on the iliac crest, terminal iliac process and the caudal ischium (i.e. around the dorsal perimeter of the pelvis) and insert onto an aponeurosis attached to the tibiotarsus, patella (and its ligament) and the knee joint capsule (2). Despite similar gross anatomy, the two heads show completely out-of-phase activity in birds, with the ILPR firing in late stance to late swing phase, whilst the ILPO is active late swing to late stance phase (2). This difference in activity likely relates to their different moment arms and mechanics around the hip joint. There are numerous other examples of a "de-coupling" of anatomical form and neuromuscular function in vertebrates that require caution in such form-function inferences (3).

Better understanding of the relationships between morphology and muscle activity will enable prediction of function for animals (whether extant or extinct) for which no data exist. Such predictions are particularly important for lineages characterized by major losses of functional disparity, such as the Archosauria ("ruling reptiles"; Crocodylia, birds/Aves, and all descendants of their most recent common ancestor); for such clades there is a need to better predict function from form. Archosauria is a clade that diversified first during Triassic period ~250 Mya, evolving a wide variety of forms including small- and large-bodied, sprawling/erect-limbed, quadrupedal/bipedal,

aquatic/amphibious/terrestrial and flightless/flying. EMG data from extant archosaurs have been used to infer locomotor changes across Archosauria as a whole (2,4,5). As EMG data are invasive and so often not feasible in extant animals, they are valuable when available, and further EMG data from extant archosaurs (different species, and different muscles than in prior studies) would aid generalization of patterns and inferences based on non-invasive data such as anatomy and kinematics.

Probably because of the difficulties inherent in collecting EMG data from appendicular muscles during locomotion, only a small range of non-mammalian amniote taxa have been studied, particularly birds (2,5–8), but also alligators (5,9–11), caiman (5), turtles (12,13), and lizards (14–18) but for each of these major groups the studies tended to focus on a small selection within the clade. For example, available hindlimb EMG data for birds are restricted to guineafowl (e.g. (2,7,8,19,20)) and domestic chickens (e.g.(6,21)), but some data exist for wild turkeys (1). These data have revealed some consistent patterns of muscle activity including co-activation of muscle pairs (e.g. M. flexor cruris lateralis pars pelvica (hip extension and knee flexion) and M. gastrocnemius pars lateralis (knee flexion and ankle extension)) (8). These avian taxa all belong to the clade Galliformes, and are studied because they are relatively terrestrial and athletic compared to many other species belonging to the speciose avian clade Neognathae. However, there have been no hindlimb EMG studies of the sister group of Neognathae, the Palaeognathae. The palaeognaths include highly specialized, terrestrial, long-limbed (cursorial) forms such as ostriches, emus, rheas, cassowaries and kiwis, but also the tinamous. Tinamous are of particular interest because they are more similar to “ancestral avian” morphology compared to other paleognaths, with small body size and retained flight capability, and are perhaps even more plesiomorphic in locomotor function than many galliforms (22).

Here, we present hindlimb EMG data during walking and running from two Palaeognathae species: Elegant-crested tinamous (*Eudromia elegans*) and emus (*Dromaius novaehollandiae*), and four galliform species: helmeted guineafowl (*Numida meleagris*), common pheasant (*Phasianus colchicus*), wild American turkey (*Meleagris gallopavo*) and bobwhite quail (*Colinus virginianus*). Additionally, we provide an ontogenetic perspective for the emus from young birds (< 4kg) to adults (>30kg) to compare post-hatching neuromuscular control, for comparison with existing data on ontogenetic scaling of limb muscles (23) and ontogenetic changes of EMG patterns in chickens (24). Finally, we broaden our study's perspective to cover extant Archosauria by including novel EMG data from Nile crocodiles (*Crocodylus niloticus*) moving both overground and on treadmills. We consider the overall patterns in muscle activity revealed by this extensive dataset to revisit the questions raised by Gatesy (3) about how much diversity exists in the neuromuscular control of locomotion among archosaurs.

Methods

All species, numbers of individuals used, ontogenetic stage, sexes and body masses are listed in Table 1.

Ethics

EMG data collection with Nile crocodiles and Elegant-crested tinamous was conducted at the RVC Structure and Motion Laboratory under a project licence approved by the college's Ethics and Welfare committee and granted by the Home Office. The guineafowl and pheasant procedures were also conducted at the RVC Structure and Motion Laboratory under a separate project licence, approved by the college's Ethics and Welfare committee and granted by the Home Office (United Kingdom).

Bobwhite quail and wild turkey data were collected at the Concord Field Station of Harvard University, following procedures licensed and approved by the Harvard Institutional Animal Care and Use Committee in accordance with the guidelines of the National Institutes of Health and the regulations of the United States Department of Agriculture.

Surgical procedures

For all species bipolar EMG electrodes were constructed of two strands of 0.004 inch diameter platinum pure TC grade (100896) insulated by heavy poly-nylon (HPN) (California Fine Wire Company, CA, USA) soldered to a connector. The free ends of the electrodes had a staggered 1mm exposed wire region spaced 1.5mm apart. The electrodes were implanted under surgical anaesthesia appropriate for that species (see details below). Surgeries involved: 1) making skin incisions over the locations of electrode placement, 2) intramuscular implantation of fine-wire bipolar electrodes, 3) subcutaneous tunnelling of electrodes to a connector on the dorsum or proximal hindlimb, 4) closure of incisions and 5) peri- and post-operative administration of analgesia. The muscles we obtained data from are shown in Tables 2 and 3.

Nile Crocodiles

The anaesthetic procedure is covered in detail in Monticelli et al., (25), but is briefly outlined here. General anaesthesia was induced using a combination of medetomidine (Sedastart, Animalcare UK; 0.2 mg kg^{-1}) and ketamine (Ketamidor, Chanelle UK; 10 mg kg^{-1}) intramuscularly in the left triceps brachii muscle. After anaesthetic induction, the crocodiles were intubated using an uncuffed endotracheal tube and anaesthesia was maintained using sevoflurane (SevoFlo, Zoetis, BE) in oxygen. Intramuscular meloxicam (Metacam, Boehringer Ingelheim, DE; 0.2 mg/kg) was administered in the perioperative period. Active warming was provided by either HotDog® or Bair Hugger® systems.

Five incisions, 1-2cm long, were made over the right ilium, anterolateral aspect of the tail, cranial thigh, caudal and cranial aspects of the lateral shank to enable visualisation and intramuscular implantation for the four hindlimb implants. A further six incisions were made to access four forelimb muscles, with incisions at the scapula, anterior and posterior aspects of the upper arm, medial aspect of the lower arm, lateral aspect of the thorax, and ventral aspect of the thorax. These incisions and subsequent electrode implantations originally targeted, respectively, for the hindlimb (after the pelvis incision, used for threading wires to the limbs): M. caudofemoralis longus, M. iliotibialis 2, M. flexor tibialis externus, and M. gastrocnemius externus and; and for the forelimb: (after the scapular incision) the M. pectoralis, M. triceps brachii (caput coracoideus), M. biceps brachii, and M. flexor digitorum longus. Yet, from some of these muscles, we either obtained no usable or else discovered with post-mortem dissections that different muscles had been implanted. Consequently, we only focus here on four muscles with successful implantations and data collection (hindlimb: M. transversus perinei, M. iliotibialis 2, M. gastrocnemius externus, M. flexor digitorum longus; forelimb: M. pectoralis) (Figure 1).

The EMG electrode connector was anchored by suturing to two scutes near the dorsal-most incision (iliac or scapular). Each pair of electrode wires was then subcutaneously tunnelled to their respective insertion sites. Tunnelling was achieved subcutaneously using a section of size 3 (internal diameter) uncuffed PVC endotracheal tubing and a looped guide wire. The electrodes were implanted using sew-through method and secured with two simple-interrupted sutures using 3-0 vicryl to prevent both translation and rotation of the wires post-surgery. The excess wiring was pulled back through to the dorsal incisions where it was coiled and tucked back into the incision site. Each incision was then flushed with lidocaine and then closed using everted mattress stitches to prevent wound contamination in the water within the enclosures. The anaesthesia was discontinued and atipamezole (1 mg kg^{-1}) (Sedastop, Animalcare, UK) was administered intramuscularly in the left M. triceps brachii, and repeated after 30 minutes in case of residual sedation. The crocodiles were then given at least two days to recover in their enclosures before any data were collected.

Emu

Six emus were anaesthetised either using mask inhalation of 5% isoflurane for the chicks, or using intramuscular injections of xylazine (3mg/kg) and ketamine (15mg/kg) to the left lateral caudal shank muscles for the juveniles and adults. After inductions, the birds were intubated with an endotracheal tube and maintained at an adequate surgical anaesthetic plane with a variable concentration of inhaled isoflurane. Breathing, heart rate and body temperature were monitored throughout surgery. The feathers in the surgical field were clipped and incisions were made for electrode implantation. The EMG electrodes were successfully implanted into M. Iliotrochantericus caudalis, M. iliotibialis lateralis pars postacetabularis, M. iliofibularis and M. gastrocnemialis pars lateralis (Figure 2). All wires exited via a skin incision caudal to the femoral trochanteric crest of the right pelvic limb. After surgery, animals were rested in their habitual pen and administered non-steroidal anti-inflammatories (meloxicam 1.5mg/kg, three times a day) until data collection was completed. Birds were assessed for discomfort before and throughout data collection; which started 24 hours post-surgery; studies were postponed or interrupted if the animals appeared distressed or lame.

Other birds

The guineafowl, pheasant, quail and turkey all underwent surgical procedures that have been described previously (26–28) with the birds anaesthetised using isoflurane delivered via a mask. The tinamous followed a similar method (see supplementary information for a more detailed protocol), although general anaesthesia was induced using intramuscular injection of 0.075 mg/kg Ketamine (Ketamidor, Chanelle UK) and 22mg/kg medetomidine (Sedastart, Animalcare UK) into the right pectoral muscle, and maintained using inhaled sevoflurane using a non-cuffed endotracheal tube

throughout the remainder of the procedure. The surgical field was plucked of feathers and sterilised and incisions made over the target muscles. The EMG electrodes were then implanted into the target muscles, while connected to a micro-connector placed on the bird's back. The electrode leads were passed subcutaneously from 1-2cm incision over the synsacrum to the larger primary incision (4-5cm) over the right lateral shank. Bipolar electrodes were constructed of 0.1mm diameter silver fine-wire (California Fine Wire, Inc., Grover Beach, USA) with 0.5-1.0mm bared tips, and 5-8mm spacing. Electrodes were emplaced using a 23 gauge hypodermic needle, and secured to the muscle using 5-0 silk suture; then skin incisions were closed using 3-0 silk. The birds were given analgesia every 12 hours and antibiotics every 24 hours. Experimental recordings took place over the next 1–3 days for most birds, but the tinamous were given six days to recover due to their potential sensitivity to stress.

For all birds the M. gastrocnemius pars lateralis was targeted, the guineafowl and turkey both had the M. flexor digitorum IV, and individually the turkey had M. flexor cruris lateralis pars pevlica, and guineafowl the M. femorotibialis lateralis. In addition to the M. gastrocnemius l pars ateralis in the tinamous, the M. iliofibularis, M. iliotibialis cranialis, and M. tibialis cranialis were targeted, but some of the channels provided no data, and after experiments were completed and the birds were euthanised, some different muscles had been implanted. Thus, we focus on the muscles for which data were successfully collected: M. gastrocnemius pars lateralis and M. fibularis longus (Figure 2).

Experimental protocol

The crocodiles were captured from their enclosures and their mouths were taped to prevent injury to themselves or handlers, or damaging their EMG wires. The crocodiles were then either placed on a Starkerhund treadmill (Terraglione di Vigodarzere, Italy) (within an acrylic-sided enclosure to

prevent the animals escaping), or on a custom wooden runway (0.38x0.40x2.44m). Previous research has shown that there should only be minor differences in EMG signals between runway and treadmill locomotion(6)'. Both the treadmill enclosure and custom wooden runway had openings in the roof to allow the wires to exit through to be connected to the EMG amplifiers. The crocodiles were motivated to walk by stimulating the tail with a broom as needed. The trials were initiated using a trigger system that created a short light flash that could be seen by the two Hero 3+ GoPro cameras (San Mateo, California) recording at 60Hz which were used to capture the footfall patterns of the animals during locomotion. Trials were maximally 60s long, although usually far shorter, with at least 60s recovery between trials. Across four individuals, a total of 160 trials were collected, with details of collected data in Table 4.

The tinamous were placed on a treadmill within a box (as above) with transparent acrylic sides to allow visualisation of the footfalls, and which had an opening for the EMG wires. Trials ranged from 30s to 60s, with at least a 60s break between trials. The treadmill speed varied from 0.1ms^{-1} to 0.45ms^{-1}; faster speeds were not safely achievable with the birds. The trial lengths and recovery were the same as the crocodiles. The birds were in the experimental area for a maximum of 1hr before being returned to their enclosure. Details of the hardware are the same as above. A total of 64 trials were collected for the two individuals, with the resulting data summarised in Table 5.

Emu trials were conducted overground in a corridor of ~90cm width enclosed by wire netting for the younger individuals, and metal fencing for the adults. Due to the wired EMG implants, cable length limited the maximum length of the runway. Cable length was ~5m for the youngest birds and 9m for the two older groups. All wires were tethered along a sliding pulley system (suspended >1m off the ground) which kept the implant cables from dragging on the floor and interfering with gait. The floor of the runway was instrumented with eight Kistler forceplates (0.6x0.9m; model 9287B, Hook, Hampshire, UK), which were used to obtain timings of footfalls. The emus were also marked with infrared-reflective tape (Scotchlite 8850; 3M, Manchester, UK) covered with polystyrene

hemispheres (1cm diameter for the youngest, 2cm diameter for the older individuals) for joint motion analysis for another study (29)), which included two dorsal midline markers used here for obtaining locomotor velocities via a Qualisys Oqus 500 six-camera system recording at 250Hz (Qualisys AB, Göteborg, Sweden). Across the six individuals 405 trials were completed, and the resulting trials are listed in Table 6.

The turkey (2 individuals, 5 trials), quail (2 individuals, 6 trials) guineafowl (2 individuals, 6 trials), and pheasant (1 individual, 1 trial) all ran on a custom-built treadmill, with a slatted black rubber-coated steel belt with a 55.8×172.7 cm running surface. The speeds were to achieve an approximately similar Froude number (see below) of 1.25 across species (Table 5). The turkey, quail and quineafowl were recorded using a Photron camera at 125Hz, whilst the pheasant was recorded using Qualisys cameras at 125Hz.

EMG recordings

Each of the sockets on the animals was connected via lightweight shielded cables to GRASS pre-amplifiers (P511. Natus Neurology Incorporated). EMG signals remained at a constant amplification throughout data collection with a low-pass (10Hz for most birds; 30Hz for emus, tinamous and crocodiles) and a high-pass (10kHz) filter. The EMG signals were sampled at 2500Hz (emu) or 5000Hz (all other species).

Data processing

Footfall events (foot on and off times) were manually recorded from the videos for the crocodiles, tinamous, guineafowl, quail, turkey and pheasant for each trial. The emu footfall timing pattern was determined by analysing the forceplate data, with foot on and off timings linked to the force traces (recorded at 1000Hz; automatically filtered using a low-pass filter at 100Hz; threshold for foot-on/off

events = 1 % body weight). Custom scripts in Matlab software (MathWorks, Natick, Massachusetts) were used for all post-processing.

The tinamous and crocodiles on the treadmill moved at three different speeds, the lowest being manually driven by a drill, the other two (0.5, 0.7mph) driven by the treadmill motor. The belt speed was calibrated from a video based on the movement of a mark on the treadmill belt relative to a point at a known distance on the treadmill frame. For the crocodiles on the runway, locomotor speed was measured by tracking the shoulder scutes (which had the least lateral movement relative to direction of movement) across 20cm, using a dorsally placed camera in the runway. Emu speeds were calculated by tracking the cranial dorsal marker in 3D space and extracting the horizontal component.

Data were then cut into individual steps based on footfall timings extracted from video or forceplate data from each species, described above. Each EMG sequence was filtered using a Butterworth filter (see Figures 3 and 4 for representative data) and then rectified. Rectified sequences were analysed using custom Matlab scripts to process the EMG signals relative to footfall timings. In species with multiple speeds, the square root of the Froude number (30) was used to normalize speed to a dimensionless quantity for comparisons:

$$u = \frac{v}{\sqrt{(g \cdot l)}}$$

where *u* is dimensionless speed, *v* is velocity, *g* is acceleration due to gravity (9.81ms^{-2}) and *l* is standing (or mid-stance) hip height. Dimensionless speed usually assumes geometric similarity (30), however dimensionless speed holds reasonably well across animals that use similar locomotor modes even if not strictly geometrically similar (see (31) and references therein for a thorough review).

As the emu trials spanned the largest range in dimensionless speeds they were grouped into 0.2*u* bins from 0.3-1.5*u*. These bins covered all of the ontogenetic ranges of the emu and overlapped with the recorded speed range of other studied bird species except for the tinamou, which never reached a dimensionless speed greater than 0.3. The crocodiles' speeds were also normalised to dimensionless speed where *l* is total hindlimb length instead of hip height due to the variety of postures (from sprawling to upright) that they used. Due to the small sample sizes in terms of both numbers of individuals and number of trials, no quantitative statistics were undertaken.

Results

Crocodiles (Figure 5)

PEC

The M. pectoralis for the Nile crocodiles showed low-level activation through mid-stance phase, with the maximum activation in late stance. Unlike the TP (below), the pattern was not shifted earlier in the cycle at higher speeds, but did result in a relatively shorter period of activation. For relatively similar speeds, there was no apparent difference between EMG signals for animals on treadmill or runways.

TP

The M. transversus perinei was active through early to mid-stance, with peak activity from 20-50% of the stride cycle. At faster speeds, the TP became active earlier, including late swing phase (FIG).

IT2

The M. iliotibialis 2 was active throughout most of the stance phase, with the greatest signals around 30% of total stride cycle (duty factor 0.74).

GE

At 0.35-0.45ms^{-1}, the M. gastrocnemius externus was active during mid-late stance, becoming active into early swing phase at the faster speeds.

Birds

Emus

There were no major differences between the age groups in terms of muscle activations. However, the baby emus may have had a slightly broader range of activations for each muscle group relative to the older individuals. With so few individuals, it is difficult to resolve whether this difference relates to individual variance or age.

ITC (Figure 6)

The M. iliotrochantericus caudalis also followed a very similar pattern to the lateral gastrocnemius, with activation during early stance, but extending through late swing and middle stance. However, at slower relative speeds the late swing and early stance activations were at lower levels, and the peak activation occurred during mid-stance. At the fastest speeds, the activation peaked in early stance.

ILPO (Figure S1)

The M. iliotibialis lateralis pars postacetabularis had variable activation with speed. At slower speeds, the EMG signals occurred at a fairly consistent level of activity from the end of swing through late-middle stance. At faster relative speeds (0.7-0.9 *u*), a peak in signal was found during mid-stance with reducing activity extending from late swing through later stance. At the fastest speeds (0.9-1.1 and 1.1-1.3 *u*), there seems to have been a discontinuity between the signal in late swing and the large peak at mid-stance; consistent with potentially two bursts of activity.

ILFB (Figure S2)

The M. iliofibularis followed a very similar pattern to the GL, with peak activation during early stance, but extending through late swing and middle stance.

GL (Figure 7)

The M. gastrocnemius pars lateralis of emus was active from late swing through middle stance at most speeds. In the youngest emus, the activity extended through stance and into early swing at *u* from 0.3-0.5. At higher values of *u*, the initial muscle activations for all ages became increasingly earlier, so activation occurred more consistently during late swing and ended earlier in stance, with higher relative activations and a smaller range as a proportion of total stride time.

Tinamous (Figure 8)

GL

Overall the M. gastrocnemius pars lateralis EMG signals were similar across the small range in speeds, with activity beginning late swing and continuing through early stance, with reduced mid-late stance signal at higher speeds.

FL

From the one trial at 0.1ms^{-1} (0.06*u* - a very slow walk) that data could be collected for, the M. fibularis longus showed low level EMG activity from foot on through to late-middle stance.

Other birds

GL

Across the quail, pheasants, guineafowl and turkey, the lateral gastrocnemius showed a similar overall pattern of activity with the primary burst of muscle activity burst occurring from late swing to early mid-stance, with peak activity early in stance (Figure 9A-D)

DFIV

The digital flexor to the fourth toe was measured in turkeys and guineafowl, and showed activity from late swing through early stance, with timing similar to that of the GL (Figures 10 and 11)

FCLP

The M. flexor cruris lateralis pars pelvica was only measured in turkeys, and was active through stance, with a peak in mid-stance (Figure 10)

FMTL

The M. femorotibialis lateralis was only measured in the guineafowl, and was active from late swing through to late stance (Figure 11).

Discussion

Here we have presented a compilation of the largest dataset of electromyographic data for archosaurs to date, including the first for emus and tinamous, thus adding palaeognathous birds to the existing literature for birds and Nile crocodiles to the published data for Crocodylia. Below, we consider our crocodylian EMG data first, then the avian data, then all data in the context of archosaurian neuromuscular evolution.

As in previous studies, regardless of whether the animal was moving within a runway or on a treadmill, the activation patterns were very similar, although the range of speeds assessed was very low, only occurring at 0.1ms^{-1} for the crocodiles, which was approximately their natural walking speed. Previously published data for Crocodylia derive entirely from the American alligator (*Alligator mississippiensis*) and spectacled caiman (*Caiman crocodilus*) hindlimb (10); in both cases for the Alligatoroidea lineage, whereas here we provide comparable data for the Crocodyloidea lineage (and forelimb PEC muscle EMG). The M. iliotibialis 2 (IT2) of Nile crocodiles had a relatively larger EMG signal than seen in alligators but it occurred with the same timing around mid-stance (11). Whilst no filtered signals are published for the M. gastrocnemius externus (GE), summarized timings (10) match very well with the signals seen in the Nile crocodile data at 0.345ms^{-1} presented here despite being different duty factors (0.6 here vs. 0.7 in (10)).

The M. transversus perinei (TP) overlies the M. caudofemoralis longus (CFL) in Crocodylia (32–34) and has similar signal patterns in terms of patterns and timings (11). Its activity has not been measured before, to our knowledge, in Reptilia. The TP is very thin and our electrodes may have

been picking up “cross-talk” signals from the CFL, which is one of the major locomotor muscles in the hindlimb (11). An alternate explanation is that the TP may have been contracting simultaneously with the CFL. The two muscles also have muscle fibres that run perpendicular to each other (TP dorsoventrally, CFL craniocaudally). Perhaps the TP performs some function of locomotor relevance, limiting bulging of the distal CFL belly near where it narrows into its insertion, or similar to the M. caudofemoralis brevis helping to change the moment arm of the CFL in lizards (35).

There are no other published forelimb EMG data for Crocodylia; however, some data exist for the Savannah monitor lizard (*Varanus exanthematicus*) (14). The M. pectoralis in this more sprawling reptile tends to be variably active, with the cranial portions active predominantly in swing phase, whilst the middle of the M. pectoralis was shown to be active at low levels during stance phase. In our Nile crocodile subject, the electrode was inserted into the cranial (i.e. major sternal) portion of the PEC, but had activity through mid-to-late stance. This difference between the two species might relate to their differences in forelimb posture, with the crocodiles adopting “high walks” in the trials reported here and potentially activating far more of their PEC maintaining this posture (i.e. resisting glenohumeral abduction imposed by ground reaction forces).

Published hindlimb EMG data from birds to date have focused primarily on guineafowl (*Numida*) and domestic chickens (2,6,8). The guineafowl data presented here compare well with the previously published guineafowl data, both in terms of patterns and timings for the GL and DFIV muscles; giving confidence to our results (2,28). Whilst variation in EMG signals through ontogeny has been found *in ovo* (e.g. (36)), very little research has been done post-hatching as the neural controls appear to establish early within embryos. However, for pectoralis muscle EMG signals during wing-assisted incline running in chukars (*Alectoris chukar*), variation in patterns exists between young and adult birds, with younger birds having longer periods of activation of their muscles relative to the adults

(37). This pattern reflects what was found within the emu leg muscles, with younger birds having generally longer activation times. A previous study of how muscle activity varied across a range of speeds in guineafowl (focussed on the ILPO), showed that muscle activity tended to reduce in relative duration with increasing speeds (38), which we have also found here across the emu muscles, and the crocodile PEC.

A recent musculoskeletal simulation study of an ostrich (39) predicted muscle activations for walking and running, but because no EMG data exists for ostriches, previous analysis has relied on comparisons with neognath EMG data. The simulation's activations generally match the additional palaeognath EMG data we present here, with the exception of the ITC(p) which in the simulation had a secondary activation during swing phase. Whilst some small peaks are found in our ITC data for the adult emus around foot-off at lower speeds, this is likely a result of noise, and no peaks indicative of secondary activations in mid-swing are found for running emus (u >1.0) (Figures). This discrepancy between the simulated muscle activations and EMG data was also found when compared to guineafowl data (22).

The M. gastrocnemius pars lateralis (GL) is most widely studied across avian species, and is useful as a reference muscle because it retains generally similar anatomy and locomotor function in terrestrial gait across species. Here we find that the GL's EMG activity patterns of the palaeognathous birds patterns are almost exactly the same as those for the neognaths (Figure 9). We suggest that across cursorial, terrestrial birds as a whole, muscle activations patterns are likely to be conserved for morphologically and functionally similar muscles. This supports the inference that these motor patterns are ancestral, at least for crown-group Aves, although as we note above there may be differences in timing during stance phase that correlate with differences limb posture and function. Nonetheless, EMG activity patterns for the GL in the mallard duck (*Anas platyrhynchos*) are similar to

the species reported here, despite morphological and functional differences associated with a more aquatically specialized lifestyle (40). Thus, GL muscle activation patterns appear to be generally conserved across Aves and correspond to the expected functional demands inferred from anatomical origins, insertions, joint mobility and moment arms.

What, then, do our EMG data indicate about the evolution of muscle activity in the clade Archosauria? There are scarce overlapping and ideally comparable data, major differences in locomotor biomechanics and some issues with muscle homology (3) that are cause for caution. Yet Crocodylia (represented by our new data for *Crocodylus niloticus*) and Aves both activate M. pectoralis during their major antigravity functions (i.e. stance phase for the former; downstroke of flight for the latter) (41) and this activity is shared with Squamata (*Varanus exanthematicus*), consistent with some "neuromotor conservation" at least across the broader amniote clade Sauria (10). This apparent conservatism of activity would support the inference that quadrupedal archosaurs used their PEC muscles to support themselves during locomotion, much as their M. adductor femoris muscles countered abduction of the hindlimbs (4).

Unfortunately, we did not obtain additional forelimb EMG data for Crocodylia. However, our hindlimb EMG data indicate broadly similar (albeit unsurprising) stance phase activity for GE/GL in both groups of extant archosaurs, consistent with a conserved antigravity function that would be expected perhaps even throughout Tetrapoda (e.g. felids (42), salamanders (FPC = medial gastrocnemius)(43)). This is also the case for the digital flexors (FL in the crocodile and DFIV in the guineafowl), which are also ankle extensors (plantarflexors) with antigravity functions and thus show timings similar to those seen in the GE/GL. Similarly, the IT2/ILPO (here represented by new data for *Crocodylus* and *Dromaius*) are homologous muscles for Archosauria (44) and exhibit stance phase activity (especially earlier in stance/late in swing) in this study and related literature cited above.

These data are most parsimoniously interpreted as homologous muscle activity that may be ancestral for Archosauria.

There was one potentially interesting difference in GL timing we observed for Crocodylia vs. Aves: the GE/GL muscles are active only in stance phase in the former, vs. starting activity in late swing phase in the latter. Considering their grossly similar anatomy, published differences in knee and ankle joint kinematics suggest one possible explanation: that the earlier onset of EMG activity in the avian GL is related to maintaining synchronized knee flexion and ankle dorsiflexion across the swing-stance transition (e.g. (45)), unlike in Crocodylia where there is knee extension and ankle plantarflexion from late swing to early stance phase (9–11).

Other EMG data for archosaurian hindlimb muscles are not feasible to compare directly within our dataset. The TP muscle of *Crocodylus* that we accidentally sampled rather than the CFL muscle (which surely maintained stance phase activity in early archosaurs; (46)) has barely been studied in the clade Sauria and deserves further analysis in the context of limb function. The ITC muscle of Aves is homologous with M. iliofemoralis of Crocodylia, and the palaeognath EMG data strengthen the hypothesis that there was a switch from swing to stance phase activity of this muscle complex within the clade Dinosauromorpha, perhaps concurrent with the origin of bipedalism and increased need for hip abductor-based support (rather than adductors) during stance phase (4). Likewise, the stance phase activity of M. iliofibularis for emus support the conclusion (2,10) that this muscle added a prominent stance phase burst at some point after the divergence of the dinosauromorph/avian lineage from Archosauria, albeit apparently maintaining a swing phase burst in most birds (2). Stance phase activity of M. fibularis longus (FL) in our one tinamou subject and trial offer tentative support (with other avian data; e.g.(2,5); and data for the lizard *Sceloporus*; (15)) for conserved stance phase

(and perhaps late swing phase) activity of that muscle across Sauria (like GE/GL); although EMG data for this muscle are lacking for Crocodylia.

While our data, and synthesis of data from the literature, indicate “conservatism” in muscle activation patterns across Archosauria, Sauria or even more broadly, an explanation for such patterns in terrestrial locomotion remains lacking. Past feeding studies have tended to invoke constraints imposed by central pattern generators, whereas except for some recent studies of turtles (12,13) the idea of neuromuscular conservation seems to have been abandoned for unclear reasons. The difficulty of decoupling intrinsic neural constraints (i.e. motor neurons are “hardwired” to fire in a particular pattern) from extrinsic biomechanical constraints (e.g. if only a few distal limb muscles can generate extensor (plantarflexor) “antigravity” moments around the ankle joint, then muscles such as M. gastrocnemius must tend to be conserved to have stance phase activity in locomotion, even if their potential neuronal activation is plastic in other behaviours) may be one reason for any neglect; other perspectives have cited further reasons to be wary (47,48).

Yet regardless of the cause(s) of a lack of change of motor patterns, such homology is valuable to evolutionary biomechanists. Here, we have added to other perspectives on the evolution of appendicular muscle control in archosaurs (2,4,10,46) by showing how a forelimb muscle (PEC) and several hindlimb muscles (GE/GL, FL/DFIV) have maintained similar motor patterns in extant Archosauria. This bolsters their usage in validating computer simulations; or otherwise inferring locomotor function; for taxa without available EMG data, whether they are extant archosaurs (39) or extinct. However, the evidence for changes of the motor patterns of muscles such as ITC, ILFB and FL is cause for caution (neuromotor conservation demands to be tested, not assumed; (2,5,12,13,41,47)) and cause for assembling datasets from more varied taxa and behaviours.

Contributions

JRH and MAD conceived the study. ARC, VRA, KBM, LPL and MAD all planned and performed surgeries on the animals, assisted by CA, PM and LP. ARC, VRA, KBM, LPL, MAD and JRH all carried out experiments. ARC conducted the data analysis assisted by MAD. ARC wrote the manuscript aided by JRH and MAD. All authors contributed to reviewing the manuscript and approved the final draft.

Acknowledgements

Enrico Eberhard, Peter Bishop and Jorn Cheney all provided advice on Matlab code. We thank La Ferme aux Crocodiles (Pierrelatte, France) for provision of the Nile crocodile subjects. We appreciate the support of the Biological Services Unit at RVC for animal care. We thank Russell Main, Emily Sparkes, Sandra Shefelbine and Heather Paxton for help with the experimental data collection for emus, and Jeffery Rankin and James Usherwood for input on that study. Thanks to Alison Tarbell and Sheridan Golding for assistance in quail, turkey and pheasant data collection. This study was supported by funding from The Royal Veterinary College and the European Research Council (ERC) under the European Union's Horizon 2020 research and innovation programme (grant agreement #695517).

References

1. Roberts TJ, Gabaldón AM. Interpreting muscle function from EMG: lessons learned from direct measurements of muscle force. Integr Comp Biol. 2008 Aug;48(2):312–320.
2. Gatesy SM. Guineafowl hind limb function. II: Electromyographic analysis and motor pattern evolution. J Morphol [Internet]. 1999 May 1; Available from: https://onlinelibrary.wiley.com/doi/abs/10.1002/%28SICI%291097-4687%28199905%29240%3A2%3C127%3A%3AAID-JMOR4%3E3.0.CO%3B2-Q

3. Lauder GV, Thomason JJ. On the inference of function from structure. Functional Morphology in Vertebrate Paleontology [Internet]. 1995. Available from: https://books.google.co.uk/books?hl=en&lr=&id=mWLDdT8y7yAC&oi=fnd&pg=PA1&dq=On+the+inference+of+function+from+structure&ots=fMdWt9gpae&sig=aE82YlNiRckOfW1hRfnsYu1l9pc

4. Hutchinson JR, Gatesy SM. Adductors, abductors, and the evolution of archosaur locomotion. Paleobiology. 2000 Dec;26(4):734–751.

5. Gatesy SM. Neuromuscular diversity in archosaur deep dorsal thigh muscles. Brain Behav Evol. 1994;43(1):1–14.

6. Jacobson RD, Hollyday M. A behavioral and electromyographic study of walking in the chick. J Neurophysiol. 1982 Jul;48(1):238–256.

7. Gordon JC, Rankin JW, Daley MA. How do treadmill speed and terrain visibility influence neuromuscular control of guinea fowl locomotion? J Exp Biol. 2015 Oct;218(Pt 19):3010–3022.

8. Ellerby DJ, Marsh RL. The mechanical function of linked muscles in the guinea fowl hind limb. J Exp Biol. 2010 Jul 1;213(Pt 13):2201–2208.

9. Gatesy SM. Hind limb movements of the American alligator (*Alligator mississippiensis*) and postural grades. J Zool. 1991 Aug;224(4):577–588.

10. Reilly SM, Willey JS, Biknevicius AR, Blob RW. Hindlimb function in the alligator: integrating movements, motor patterns, ground reaction forces and bone strain of terrestrial locomotion. J Exp Biol. 2005 Mar;208(Pt 6):993–1009.

11. Gatesy SM. An electromyographic analysis of hindlimb function in Alligator during terrestrial locomotion. J Morphol. 1997 Nov;234(2):197–212.

12. Rivera AR, Blob RW. Forelimb muscle function in pig-nosed turtles, Carettochelys insculpta: testing neuromotor conservation between rowing and flapping in swimming turtles. Biol Lett. 2013 Oct 23;9(5):20130471.

13. Rivera AR, Wyneken J, Blob RW. Forelimb kinematics and motor patterns of swimming loggerhead sea turtles (Caretta caretta): are motor patterns conserved in the evolution of new locomotor strategies? J Exp Biol. 2011 Oct 1;214(Pt 19):3314–3323.

14. Jenkins FA, Goslow GE. The functional anatomy of the shoulder of the savannah monitor lizard (Varanus exanthematicus). J Morphol. 1983 Feb;175(2):195–216.

15. Reilly SM. Quantitative electromyography and muscle function of the hind limb during quadrupedal running in the lizard Sceloporus clarki. ZOOLOGY-JENA- [Internet]. 1995;98:263–263. Available from: https://people.ohio.edu/reilly/pdfzacs%201995%2098%20283-277.pdf

16. Foster KL, Higham TE. Integrating gastrocnemius force-length properties, in vivo activation and operating lengths reveals how Anolis deal with ecological challenges. J Exp Biol. 2017 Mar 1;220(Pt 5):796–806.

17. Higham TE, Jayne BC. In vivo muscle activity in the hindlimb of the arboreal lizard, Chamaeleo calyptratus: general patterns and the effects of incline. J Exp Biol. 2004 Jan;207(Pt 2):249–261.

18. Foster KL, Higham TE. Context-dependent changes in motor control and kinematics during locomotion: modulation and decoupling. Proc Biol Sci. 2014 May 7;281(1782):20133331.

19. Marsh RL, Ellerby DJ, Carr JA, Henry HT, Buchanan CI. Partitioning the energetics of walking and running: swinging the limbs is expensive. Science. 2004 Jan 2;303(5654):80–83.

20. Higham TE, Biewener AA, Wakeling JM. Functional diversification within and between muscle synergists during locomotion. Biol Lett. 2008 Feb 23;4(1):41–44.

21. Bradley NS, Bekoff A. Development of coordinated movement in chicks: II. Temporal analysis of hindlimb muscle synergies at embryonic day 10 in embryos with spinal gap transections. J Neurobiol. 1992 Jun;23(4):420–432.

22. Yonezawa T, Segawa T, Mori H, Campos PF, Hongoh Y, Endo H, et al. Phylogenomics and morphology of extinct paleognaths reveal the origin and evolution of the ratites. Curr Biol. 2017 Jan 9;27(1):68–77.

23. Lamas LP, Main RP, Hutchinson JR. Ontogenetic scaling patterns and functional anatomy of the pelvic limb musculature in emus (Dromaius novaehollandiae). PeerJ. 2014 Dec 23;2:e716.

24. Bekoff A. Ontogeny of leg motor output in the chick embryo: a neural analysis. Brain Res. 1976 Apr 23;106(2):271–291.

25. Monticelli P, Ronaldson HL, Hutchinson JR, Cuff AR, d Ovidio D, Adami C. Medetomidine-ketamine-sevoflurane anaesthesia in juvenile Nile crocodiles (Crocodylus niloticus) undergoing experimental surgery. Vet Anaesth Analg. 2018 Sep;

26. Daley MA, Voloshina A, Biewener AA. The role of intrinsic muscle mechanics in the neuromuscular control of stable running in the guinea fowl. J Physiol (Lond). 2009 Jun 1;587(Pt 11):2693–2707.

27. Daley MA, Biewener AA. Leg muscles that mediate stability: mechanics and control of two distal extensor muscles during obstacle negotiation in the guinea fowl. Philos Trans R Soc Lond, B, Biol Sci. 2011 May 27;366(1570):1580–1591.

28. Daley MA, Biewener AA. Muscle force-length dynamics during level versus incline locomotion: a comparison of in vivo performance of two guinea fowl ankle extensors. J Exp Biol. 2003 Sep;206(Pt 17):2941–2958.

29. Lamas LRGP. Musculoskeletal biomechanics during growth on emu (Dromaius; Aves) : an integrative experimental and modelling analysis [Internet] [Doctoral dissertation]. Royal Veterinary College; 2015. Available from: https://ethos.bl.uk/OrderDetails.do;jsessionid=CE35DCF1E83B93B9A9AFBFEE1B05A766?uin=uk.bl.ethos.701660

30. Alexander RM, Jayes AS. A dynamic similarity hypothesis for the gaits of quadrupedal mammals. J Zool. 1983;201(1):135–152.

31. Daley MA, Birn-Jeffery A. Scaling of avian bipedal locomotion reveals independent effects of body mass and leg posture on gait. J Exp Biol. 2018 May 22;221(Pt 10).

32. Frey E. Ecology, locomotion and tail muscle anatomy of crocodiles.

33. Romer AS. Crocodilian pelvic muscles and their avian and reptilian homologues. Bulletin of the AMNH [Internet]. 1923;48(15). Available from: http://digitallibrary.amnh.org/handle/2246/1307

34. Cong L, Hou L, Wu XC, Hou JF. The gross anatomy of Alligator sinensis Fauvel.

35. Herrel ANTHONY, Vanhooydonck BIEKE, Porck JOANNE, Irschick DUNCANJ. Anatomical basis of differences in locomotor behavior in anolis lizards: A comparison between two ecomorphs. Bulletin of the Museum of Comparative Zoology. 2008 Dec;159(4):213–238.

36. Watson SJ, Bekoff A. A kinematic analysis of hindlimb motility in 9- and 10-day-old chick embryos. J Neurobiol. 1990 Jun;21(4):651–660.

37. Tobalske BW, Jackson BE, Dial KP. Ontogeny of Flight Capacity and Pectoralis Function in a Precocial Ground Bird (Alectoris chukar). Integr Comp Biol. 2017 Aug 1;57(2):217–230.

38. Carr JA, Ellerby DJ, Marsh RL. Function of a large biarticular hip and knee extensor during walking and running in guinea fowl (Numida meleagris). J Exp Biol. 2011 Oct 15;214(Pt 20):3405–3413.

39. Rankin JW, Rubenson J, Hutchinson JR. Inferring muscle functional roles of the ostrich pelvic limb during walking and running using computer optimization. J R Soc Interface. 2016;13(118).

40. Biewener AA, Corning WR. Dynamics of mallard (Anas platyrynchos) gastrocnemius function during swimming versus terrestrial locomotion. J Exp Biol. 2001 May;204(Pt 10):1745–1756.

41. Goslow GE, Wilson D, Poore SO. Neuromuscular correlates to the evolution of flapping flight in birds. Brain Behav Evol. 2000 Feb;55(2):85–99.

42. Rasmussen S, Chan AK, Goslow GE. The cat step cycle: electromyographic patterns for hindlimb muscles during posture and unrestrained locomotion. J Morphol. 1978 Mar;155(3):253–269.

43. Ashley-Ross MA. Patterns of hind limb motor output during walking in the salamander Dicamptodon tenebrosus, with comparisons to other tetrapods. J Comp Physiol A. 1995 Sep;177(3).

44. Hutchinson J. The evolution of pelvic osteology and soft tissues on the line to extant birds (Neornithes). Zool J Linn Soc. 2001 Feb;131(2):123–168.

45. Higham TE, Nelson FE. The integration of lateral gastrocnemius muscle function and kinematics in running turkeys. Zoology (Jena). 2008 Jul 26;111(6):483–493.

46. Gatesy SM. Caudefemoral Musculature and the Evolution of Theropod Locomotion. Paleobiology [Internet]. 1990;16(2):170–186. Available from: https://www.jstor.org/stable/2400918

47. Smith KK. Are neuromotor systems conserved in evolution? Brain Behav Evol. 1994;43(6):293–305.

48. Alfaro ME, Herrel A. Introduction: major issues of feeding motor control in vertebrates. Am Zool. 2001 Dec;41(6):1243–1247.

49. Allen V, Molnar J, Parker W, Pollard A, Nolan G, Hutchinson JR. Comparative architectural properties of limb muscles in Crocodylidae and Alligatoridae and their relevance to divergent use of asymmetrical gaits in extant Crocodylia. J Anat. 2014 Dec;225(6):569–582.

50. Hudson GE, Schreiweis DO, Wang SYC, Lancaster DA. A numerical study of the wing and leg muscles of tinamous Tinamidae. Northwest Science Cheney [Internet]. 1972 Feb 6; Available from: https://eurekamag.com/research/037/670/037670780.php

51. Meers MB. Crocodylian forelimb musculature and its relevance to Archosauria. Anat Rec A Discov Mol Cell Evol Biol. 2003 Oct;274(2):891–916.

52. Vanden Berge JC, Zweers GA. Myologia. In: Baumel JJ, King AS, Breazile JE, Evans HE, Vanden Berge JC, editors. Handbook of Avian Anatomy: Nomina Anatomica Avium [Internet]. Cambridge, Massachusetts, USA: Nuttal Ornithological Club; 1993. Available from: https://books.google.co.uk/books/about/Handbook_of_Avian_Anatomy.html?id=bcdKAAAAYAAJ&hl=en

Figure 1. Crocodile muscles that EMG data were collected from. A) Hindlimb dorsal view, B) Forelimb ventral view. Both right limbs, modified from (49). Muscle abbreviations in Table 2.

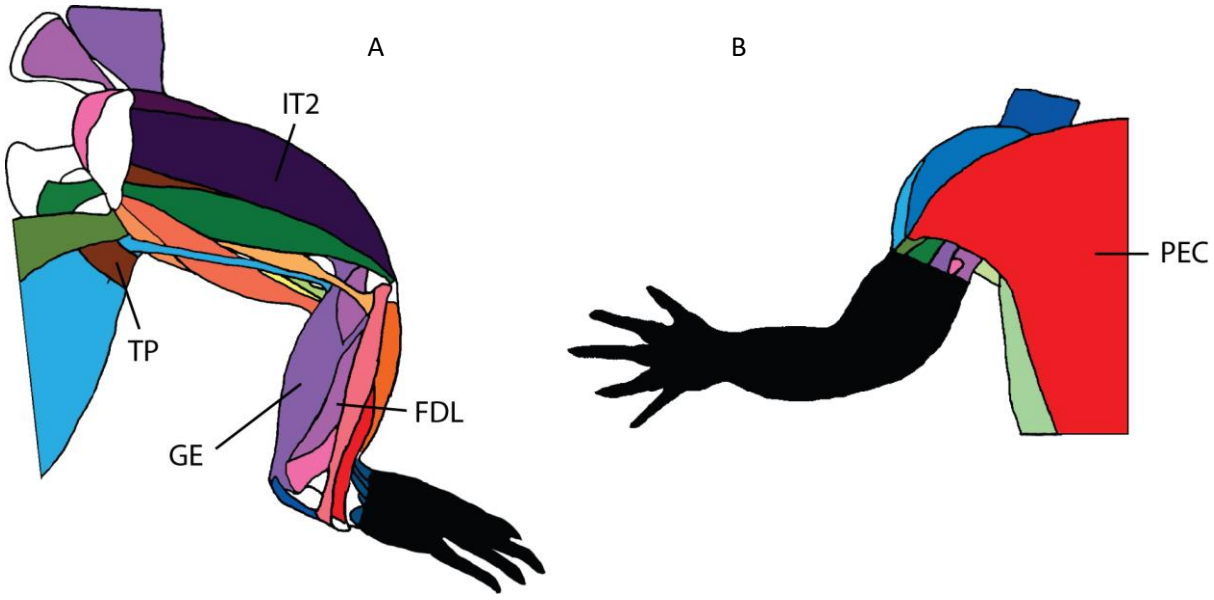

Figure 2. Avian muscles that EMG data were collected from. Hindlimb is from a representative tinamou; figure modified from (50). Muscle abbreviations from Table 3.

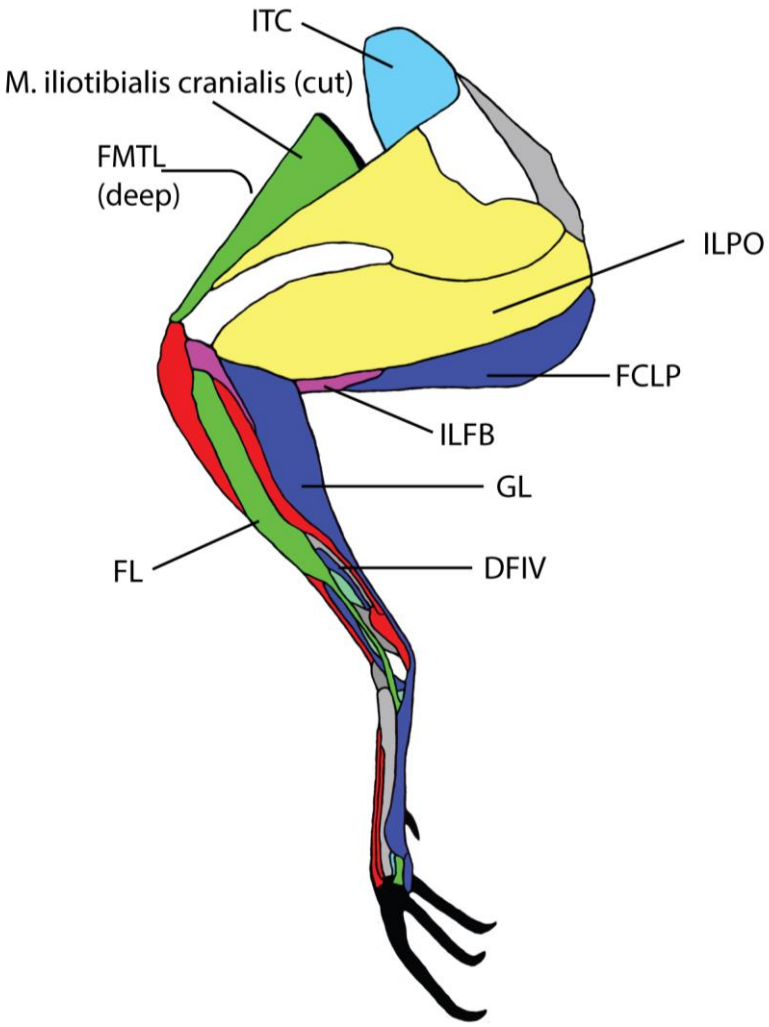

Figure 3. Filtered EMG signals from three emus at three ages, showing the signal variation at 1.1-1.3 dimensionless speed.

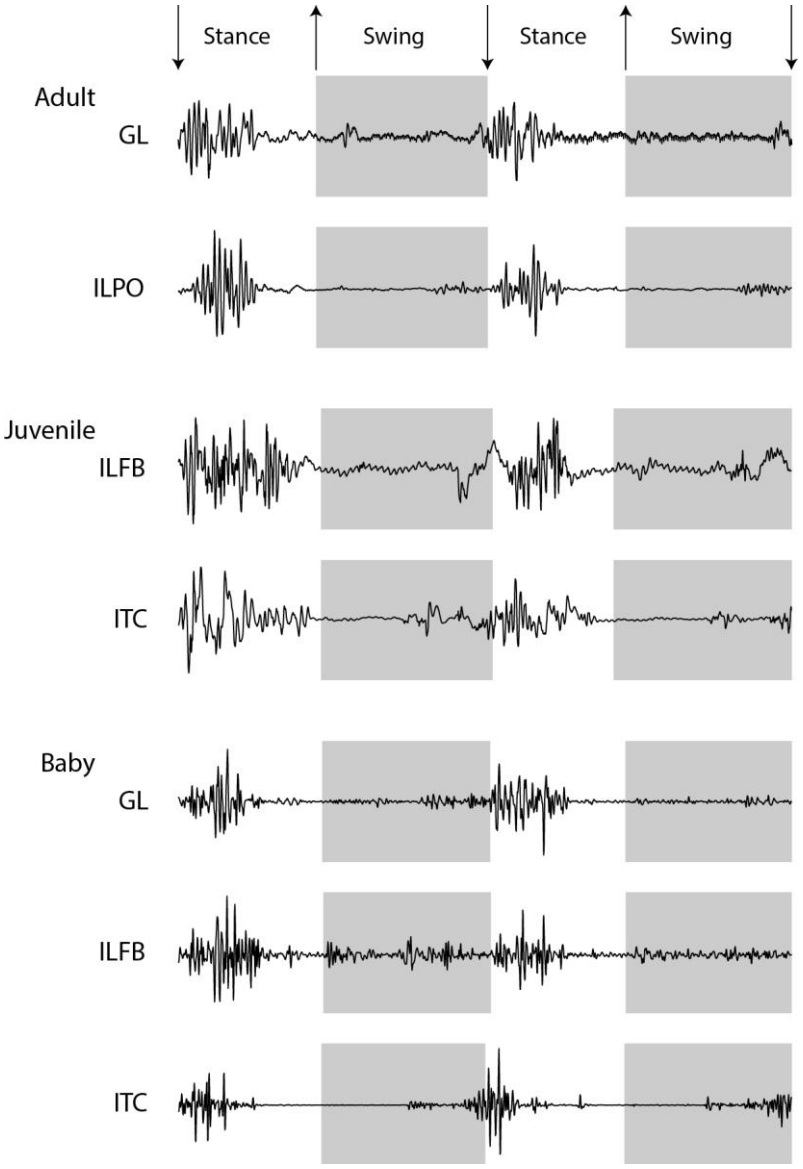

Figure 4. Filtered EMG for crocodile muscles during normal walking (~0.1 ms^{-1}).

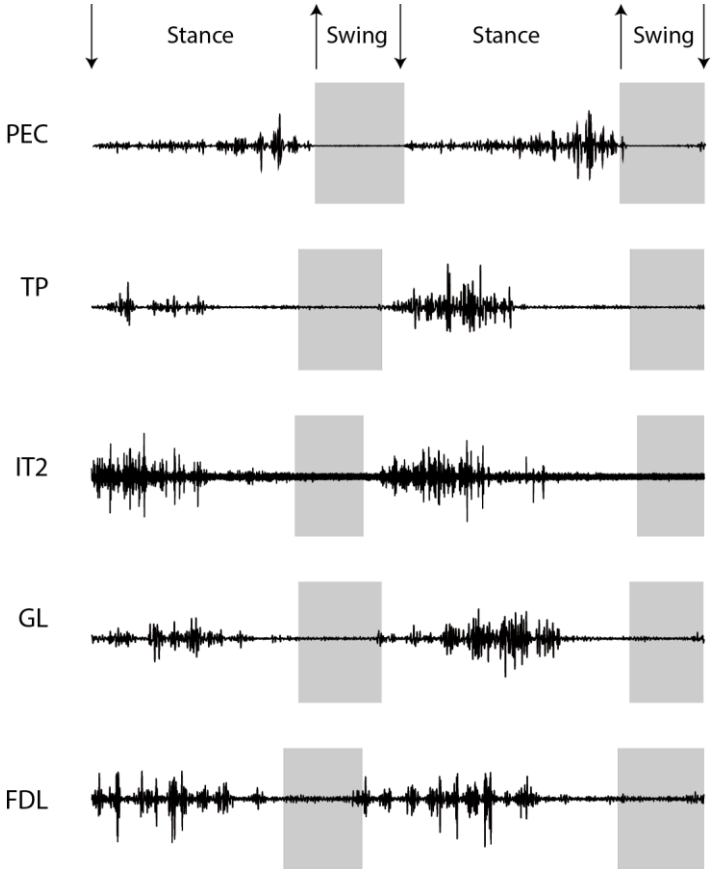

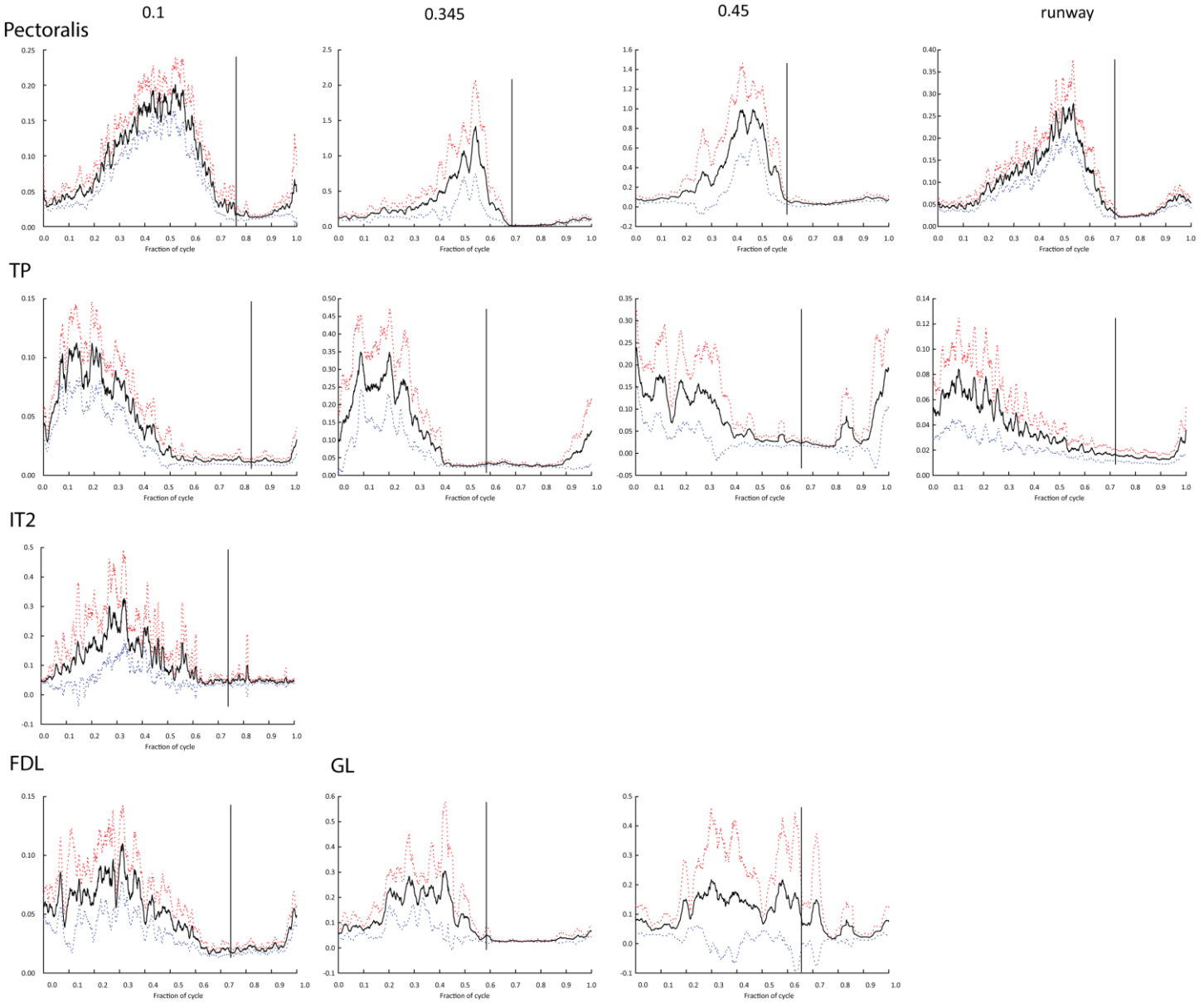

Figure 5. Crocodile EMG signals for the PEC, TP, IT2 FDL and GL muscles. Columns relate to speeds, with all speeds in ms^{-1}. The runway corresponds to normal walking speed, which was about 0.1 ms^{-1}.

Vertical lines show the average duty factor of the trials. Black = average, red and blue are upper and lower 95% confidence intervals.

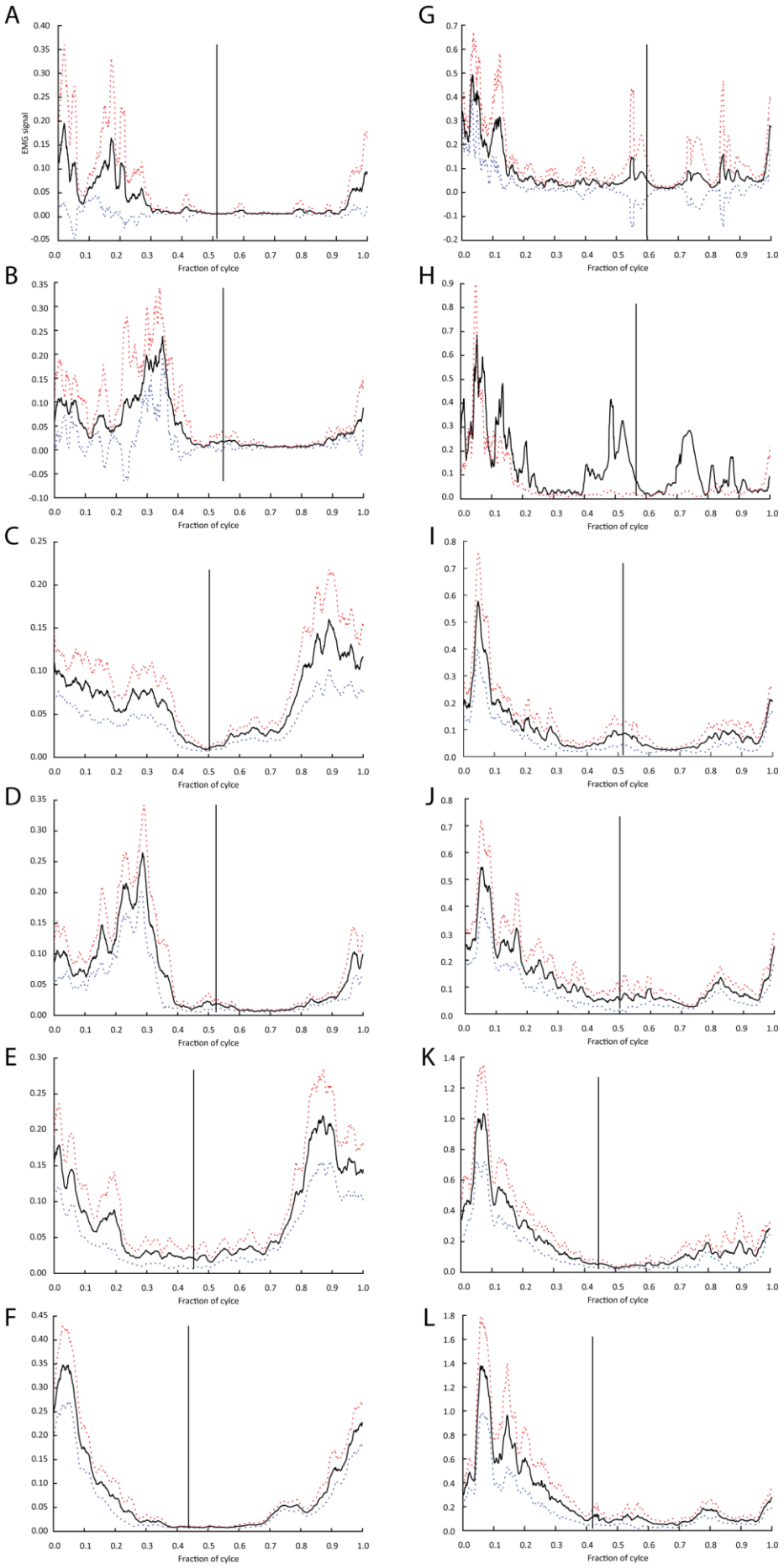

Figure 6. M. iliotrochantericus caudalis (ITC) across different speeds for emu babies and juveniles. A-F) Babies, G-L) juveniles.

AG) = 0.3-0.5*u*

BH) = 0.5-0.7*u*

CI) = 0.7-0.9*u*

DJ) = 0.9-1.1*u*

EK) = 1.1-1.3*u*

FL) = 1.3-1.5*u*

Vertical lines show the average duty factor of the trials. Black = average, red and blue are upper and lower 95% confidence intervals. Y axis is recorded electrical signal after amplification, filtering and rectification, but due to different amplifications they are not comparable between the different ages.

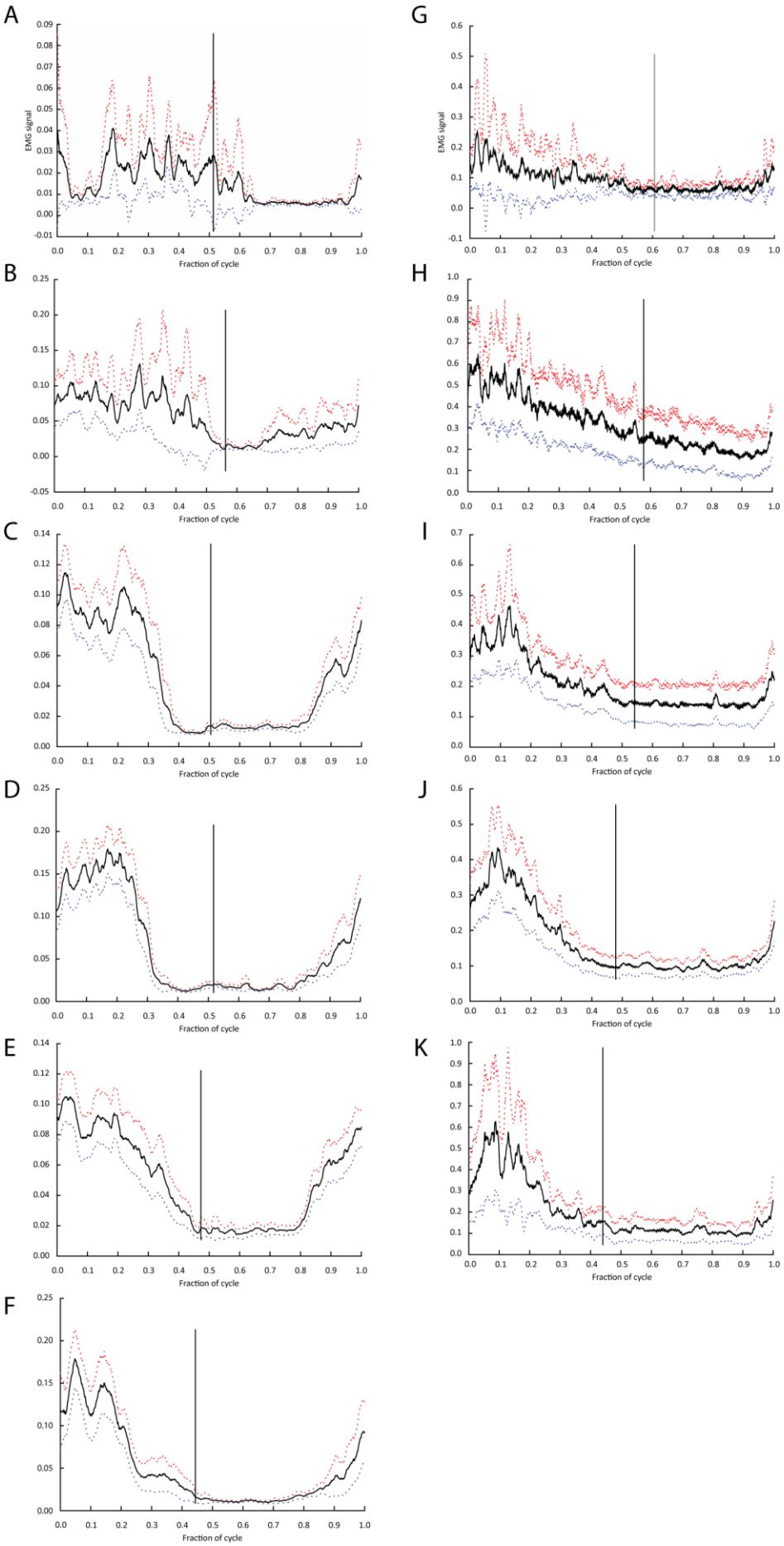

Figure 7. M. gastrocnemius pars lateralis across different speeds for emu babies and adults. A-F) Babies, G-K) Adult.

A,G) = 0.3-0.5*u*

B,H) = 0.5-0.7*u*

C,I) = 0.7-0.9*u*

D,J) = 0.9-1.1*u*

E,K) = 1.1-1.3*u*

F) = 1.3-1.5*u*

Vertical lines show the average duty factor of the trials. Black = average, red and blue are upper and lower confidence intervals. Y axis is recorded electrical signal after amplification, filtering and rectification, but due to different amplifications they are not comparable between the different ages.

Figure 8. Tinamou average EMG signals for A-C) GL, and D) FL muscles. A,D) *u* = 0.06, B) *u* = 0.23, C) *u* = 0.29. Vertical lines show the average duty factor of the trials. Black = average, red and blue are upper and lower 95% confidence intervals. Y axis is recorded electrical signal after amplification, filtering and rectification, but due to different amplifications they are not comparable between the different graphs.

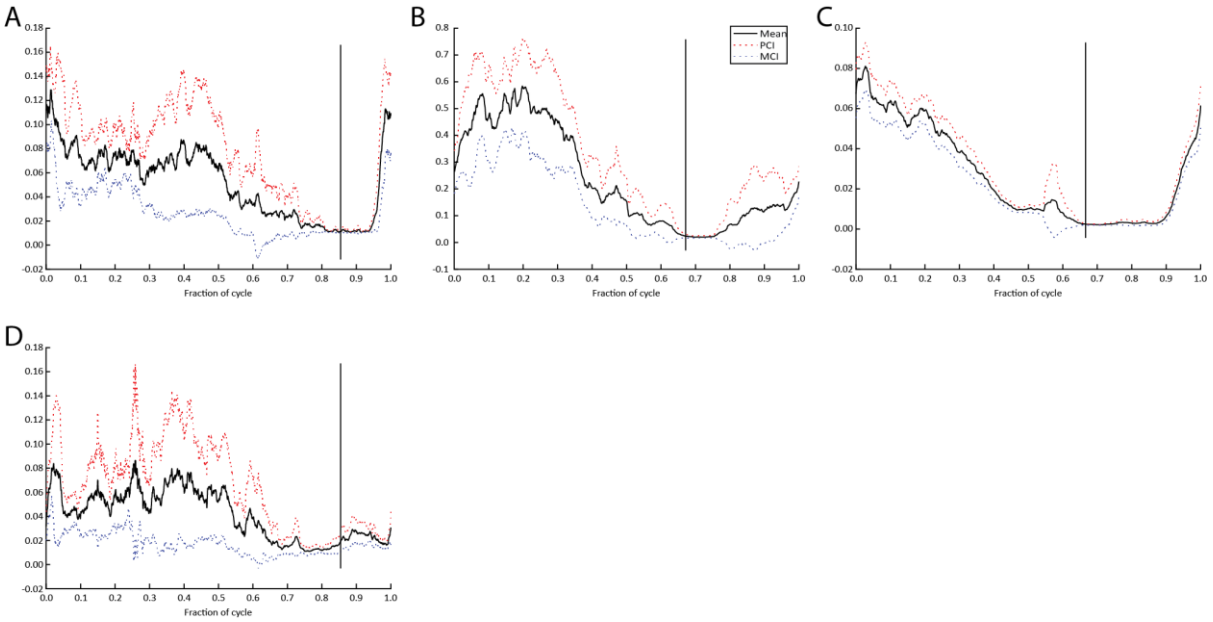

Figure 9. M. gastrocnemius pars lateralis across bird species at the same dimensionless speed (1.2). A) turkey, B) guineafowl, C) pheasant, D) quail, E) emu, F) tinamou. Vertical lines show the average duty factor of the trials. Black = average, red and blue are upper and lower 95% confidence intervals. Y axis is recorded electrical signal after amplification, filtering and rectification, but due to different amplifications are not directly comparable across species.

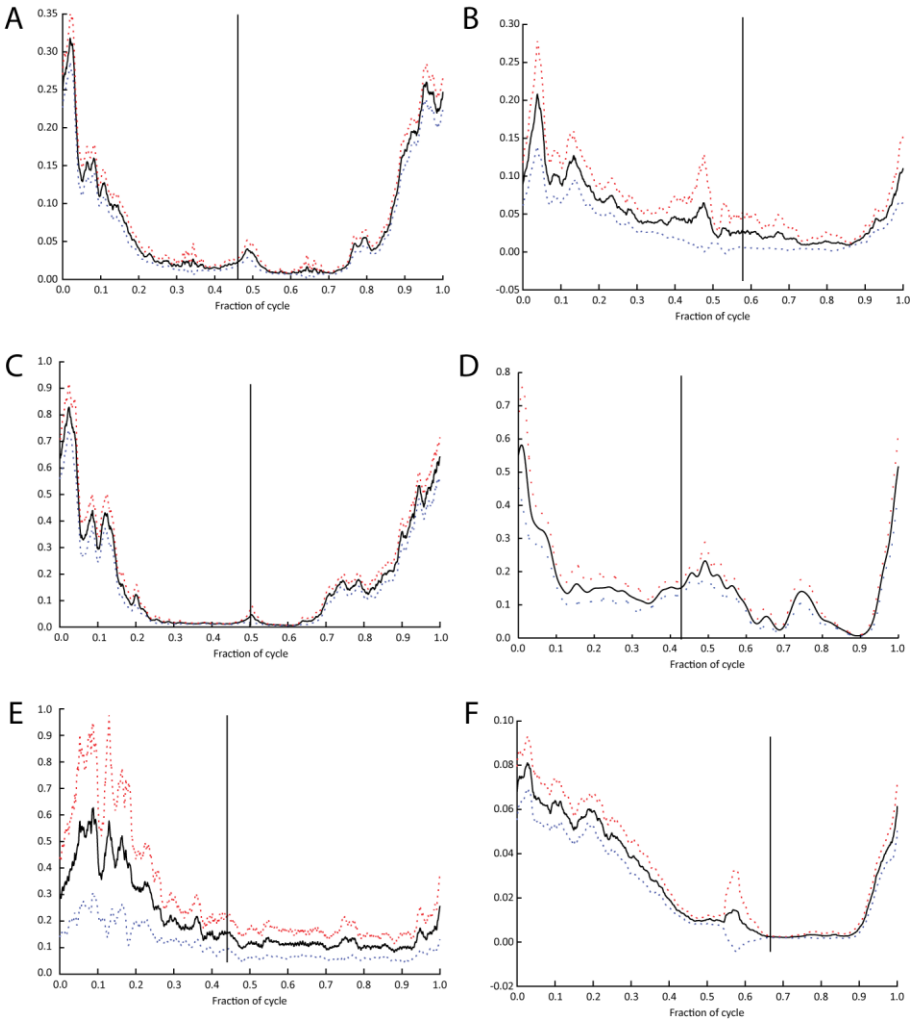

Figure 10. Turkey average EMG signals for A) FCLP, B) GL and C) DFIV muscles. Vertical lines show the average duty factor of the trials. Black = average, red and blue are upper and lower 95% confidence intervals. Y axis is recorded electrical signal after amplification, filtering and rectification, but due to different amplifications they are not comparable between the different muscles.

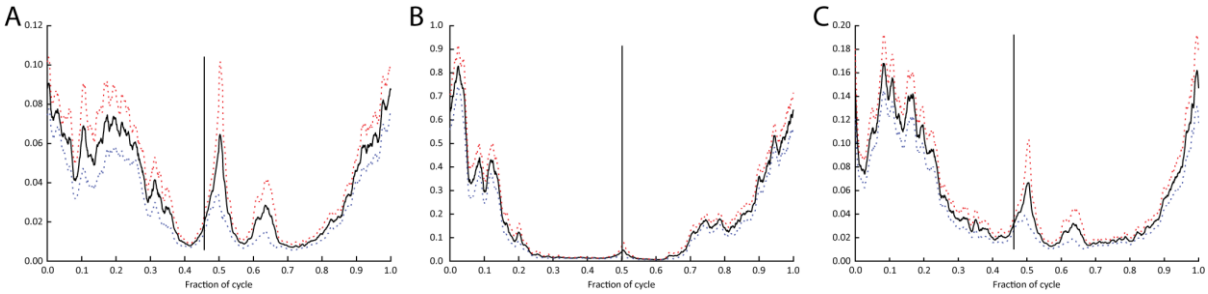

Figure 11. Guineafowl average EMG signals for A) FMTL, B) GL and C) DFIV muscles. Vertical lines show the average duty factor of the trials. Black = average, red and blue are upper and lower 95% confidence intervals. Y axis is recorded electrical signal after amplification, filtering and rectification.

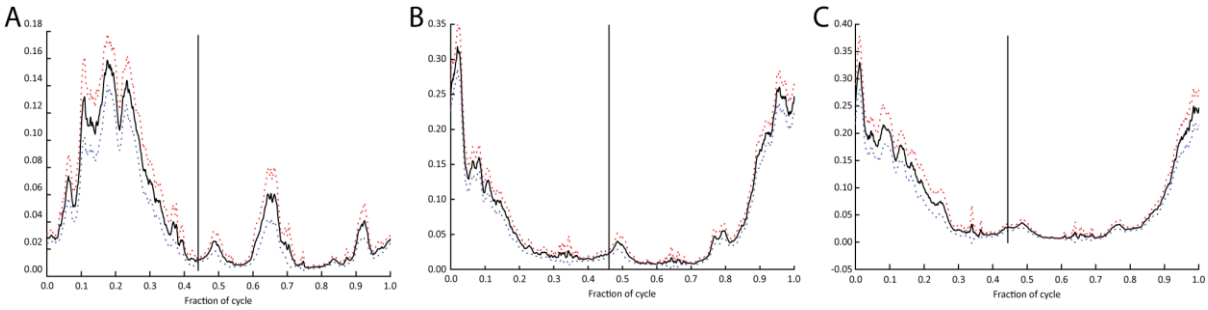

Table 1. Species used in the study

Species	Common name	Ontogenetic stage	Number of individuals	Sex	Mass (kg)
Crocodylus niloticus	Nile crocodile	Juvenile	4	F	1.59-4.63
Dromaius novaehollandiae	Emu	Baby, Juvenile, Adult	2 2 2	Unknown	3.95-4.1, 17-18, 36-37
Eudromia elegans	Elegant-crested tinamou	Adult	2	F,M	0.555-0.616
Numida meleagris	Guineafowl	Adult	2	F,M	1.5, 1.7
Phasianus colchicus	Common pheasant	Adult	2	M	1.0, 1.1
Coturnix virginianus	Bobwhite quail	Adult	2	F	0.15, 0.17
Meleagris gallopavo	Wild turkey	Adult	2	F	5.2, 6.0

Table 2. Crocodile muscles that EMG data were obtained from, with previously reported anatomy and function. Nomenclature follows Meers (51) and Allen et al. (49) and references therein for Crocodylia. “Actions” (presumed potential functions around joints crossed) are inferred from anatomy.

Muscle	**Taxon**	**Origin**	**Insertion**	**Action**
Pectoralis (PEC)	Crocodylia	Ventral surface of sternum, ribcage, surrounding area	Deltopectoral crest of humerus	Glenohumeral extensor, abductor and supinator
Transversus perinei (TP)	Crocodylia	Ischium	Centra of caudal vertebrae 1+2	Unknown: possibly shaping tail base
Iliotibialis 2 (IT2)	Crocodylia	Dorsal ilium	Cranial side of proximal tibia	Hip abductor (also long-axis rotator and flexor/extensor?); knee extensor
Gastrocnemius externus (GE)	Crocodylia	Caudal side of lateral condyle of femur	Caudal surface of proximal (tarso)metatarsus	Knee flexor; ankle extensor
Flexor digitorum longus – hindlimb (FDL)	Crocodylia	Disto-lateral femoral condyle	Distal pes	Digital flexor; ankle extensor

Table 3. Bird muscles that EMG data were obtained from, with previously reported anatomy and function. Nomenclature follows Vanden Berge and Zweers (52) for Aves. “Actions” (presumed potential functions around joints crossed) are inferred from anatomy following Vanden Berge and Zweers (52) and Lamas et al. (2014).

Muscle	Taxon	Origin	Insertion	Action
Iliotrochantericus caudalis (ITC)	Aves	Preacetabular ilium	Trochanteric crest of proximal femur	Hip flexor, abductor and internal rotator
Iliotibialis lateralis pars postacetabularis (ILPO)	Aves	Dorsal postacetabular ilium	Patella and cranial tibial crest of tibiotarsus	Hip extensor, abductor and external rotator; knee extensor
Iliofibularis (ILFB)	Aves	Postacetabular ilium	Fibula (M. iliofibularis tubercle)	Hip extensor, abductor and external rotator; knee flexor
Flexor cruris lateralis pars pelvica (FCLP)	Aves	Posterior rim of terminal iliac process	GE/GL and flexor cruris medialis tendon	Hip extensor, abductor and external rotator; knee flexor
Femorotibialis lateralis (FMTL)	Aves	Lateral surface of femur	Craniolateral surface of proximal tibiotarsus	Knee extensor
Gastrocnemius pars lateralis (GL)	Aves	Caudal side of lateral condyle of femur	Caudal surface of proximal (tarso)metatarsus (i.e. hypotarsus of birds)	Knee flexor; ankle extensor
Fibularis longus (FL)	Aves	Craniolateral surface of proximal tibiotarsus	Tarsus (with connections to digital flexor tendons)	Ankle extensor (and potentially digital flexor)
Flexor perforatus IV (DFIV)	Aves	Lateral knee ligaments	Phalanx IV of Digit IV	Ankle extensor; digit IV flexor

Table 4. Nile crocodile muscle data summary.

Species	Nile crocodile											
Muscle	TP				IT2	FDL	PEC				GL	
N individuals	1	2	1	1	1	1	1	1	1	1	1	1
Surface	Runway	Treadmill	Treadmill	Treadmill	Treadmill	Treadmill	Runway	Treadmill	Treadmill	Treadmill	Treadmill	Treadmill
Speed (ms^{-1})	0.10	0.10	0.35	0.45	0.10	0.10	0.10	0.10	0.35	0.45	0.35	0.45
u	0.07	0.07	0.26	0.33	0.07	0.07	0.07	0.07	0.26	0.33	0.26	0.33
# trials	5	9	2	2	2	5	5	4	2	2	2	2
# steps	14	25	8	7	6	16	14	19	8	9	8	7

Table 5. Bird muscle data summary.

	Tinamous				Turkey			Pheasant	Quail	Guineafowl		
Muscle	GL			FL	GL	FCLP	DFIV	GL	GL	GL	DFIV	FMTL
N individuals	1	1	1	1	2	2	2	1	2	2	2	2
Surface	Treadmill	Treadmill	Treadmill	Treadmill	Treadmill	Treadmill	Treadmill	Treadmill	Treadmill	Treadmill	Treadmill	Treadmill
Speed (ms^{-1})	0.10	0.35	0.45	0.10	2.15	2.15	2.15	1.7	1.12	1.7	1.7	1.7
u	0.06	0.23	0.29	0.06	1.27	1.27	1.27	1.25	1.23	1.28	1.28	1.28
# trials	2	2	2	2	5	5	5	1	6	6	6	6
# steps	7	7	17	7	46	46	46	14	45	54	54	54

Table 6. Emu muscle data summary for all ontogenetic stages.

Emu - baby

Muscle	GL						ILFB						ITC			
N individuals	1	1	2	1	2	2	1	1	1	1	1	1	2	1	1	1
Surface	Runway	Runway	Runway	Runway	Runway	Runway	Runway	Runway	Runway	Runway	Runway	Runway	Runway	Runway	Runway	Runway
Speed (ms^{-1})	0.6-0.92	0.92-1.3	1.3-1.7	1.7-2.0	2.0-2.4	2.4-2.7	1.3-1.7	1.7-2.0	2.0-2.4	2.4-2.7	0.6-0.92	0.92-1.3	1.3-1.7	1.7-2.0	2.0-2.4	2.4-2.7
u	0.3-0.5	0.5-0.7	0.7-0.9	0.9-1.1	1.1-1.3	1.3-1.5	0.7-0.9	0.9-1.1	1.1-1.3	1.3-1.5	0.3-0.5	0.5-0.7	0.7-0.9	0.9-1.1	1.1-1.3	1.3-1.5
# trials	2	3	11	8	19	10	7	8	9	1	2	1	9	2	10	9
# steps	6	10	43	34	81	43	26	34	40	4	6	3	31	9	41	39

Emu - juvenile

Muscle	ILFB				ITC			
N individuals	1	1	1	1	1	1	1	1
Surface	Runway	Runway	Runway	Runway	Runway	Runway	Runway	Runway
Speed (ms^{-1})	2.9-3.3	3.3-4.0	1.19-1.3	1.4-1.9	1.9-2.4	2.4-2.9	2.9-3.3	3.3-4.0
u	1.1-1.3	1.3-1.5	0.3-0.5	0.5-0.7	0.7-0.9	0.9-1.1	1.1-1.3	1.3-1.5
# trials	10	9	2	1	5	7	10	9
# steps	18	16	4	2	11	15	18	16

Emu - adult

Muscle	GL					ILPO				
N individuals	1	1	2	2	2	1	1	1	1	1
Surface	Runway	Runway	Runway	Runway	Runway	Runway	Runway	Runway	Runway	Runway
Speed (ms^{-1})	0.98-1.4	1.4-2.02	2.02-2.65	2.65-3.23	3.23-3.7	0.98-1.4	1.4-2.02	2.02-2.65	2.65-3.23	3.23-3.7
u	0.3-0.5	0.5-0.7	0.7-0.9	0.9-1.1	1.1-1.3	0.3-0.5	0.5-0.7	0.7-0.9	0.9-1.1	1.1-1.3
# trials	2	4	12	21	7	2	4	6	8	3
# steps	4	8	24	41	13	4	8	12	16	6

Supplementary information

Tinamou surgical details

General anaesthesia was induced with 22 mg/kg of ketamine (Ketamidor, Chanelle UK) and 0.075 mg/kg of medetomidine (Sedastart, Animalcare UK) administered intramuscularly in the right pectoral muscle. Once the anaesthetic induction was achieved, Tinamous were intubated with the use of an uncuffed endotracheal tube and surgical anaesthesia was then maintained with sevoflurane in oxygen. Hypothermia was limited with the use of active warming by either HotDog® or Bair Hugger® as per the crocodile surgeries. Five incisions 1-2cm long were made over the right ilium, caudal thigh, cranial thigh, caudal and cranial aspects of the lateral shank to enable visualisation and intramuscular implantation for the four implants. These incisions targeted, respectively (after the iliac incision), M. iliofibularis, M. iliotibialis cranialis, M. gastrocnemius pars lateralis, and M. tibialis cranialis. Some of the channels provided no data, and after experiments were completed and the birds were euthanised, some different muscles had been implanted, thus we focus on the muscles for which data were successfully collected: M. gastrocnemius pars lateralis and M. fibularis longus.

As with the crocodiles, the electrodes had been constructed of two strands of 0.004 inch diameter platinum pure TC grade insulated by heavy poly-nylon except soldered to a 26 pin IDC socket (625-7404 RS PRO). The IDC socket was attached to microporous surgical tape to create a backpack, through which the electrodes passed through a protective silicon tubing to the ventral aspect. A very similar method to the crocodiles was followed from here on. The free ends of electrodes were exposed and staggered. The electrode pairs were then tunnelled from the iliac incision to their respective insertion sites, with the shank implants being tunnelled via the cranial thigh incision. The electrodes were implanted using sew-through method and secured with two simple-interrupted sutures. The excess wiring was pulled back through to the iliac incision and tucked into a special pouch in the backpack. A splash block with lidocaine 0.2% (B Braun, DE) was performed for each surgical incision site prior to its closure (using 2-3 sutures of 5-0 mersilk) . The ground electrode was then injected along the midline and sutured into place. Next, the backpack was secured with eight sutures. Atropine (Atrocare, Animalcare, UK; 0.02 mg/kg) was given intravenously in the birds that experienced intraoperative bradyarrhythmias and hypotension. Occasionally, self-limited ventricular tachyarrhytmias were observed after the use of atropine. Butorphanol (Alvegesic, Dechra, AT; 2 mg/kg) and meloxicam (0.2 mg/kg) were administered intravenously to provide analgesia in the intraoperative and immediate postoperative period. At the end of the procedure, 0.1mg/kg atipamezole (Sedastop, Animalcare, UK) was given intramuscularly in the pectoralis muscle to antagonise the previously administered medetomidine. Atipamezole was redosed after 20 minutes in the birds that experienced a slow recovery. The birds were then given six days to recover before any data were collected in their enclosures, where they had access to food and water *ad libitum*.

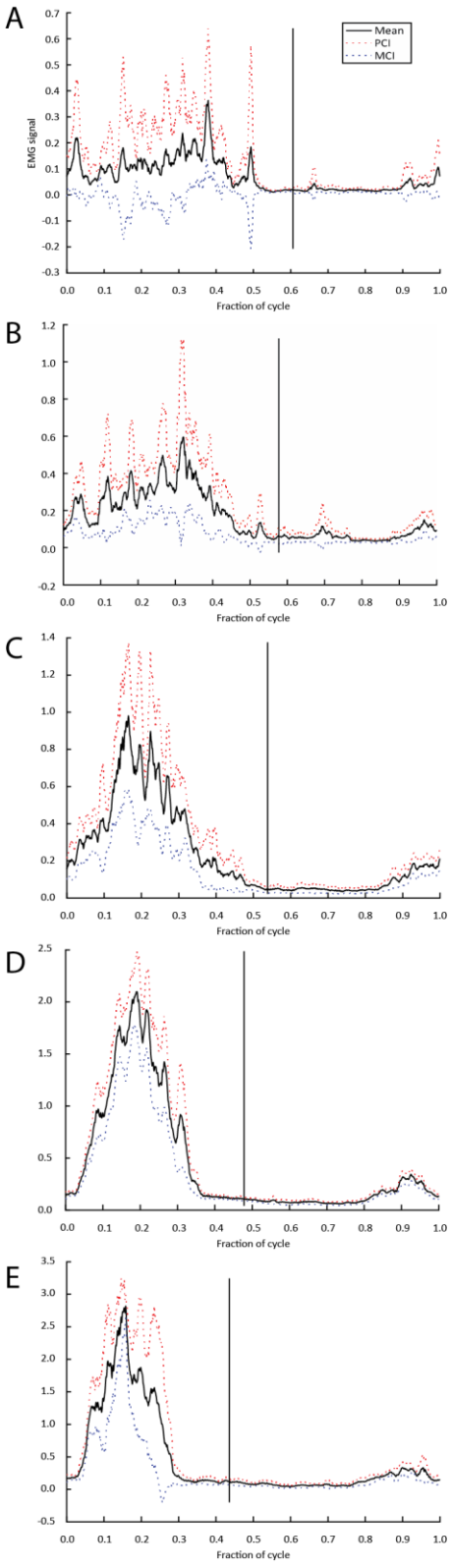

Figure S1. ILPO average EMG signals across different speeds for emu adults.

A) = 0.3-0.5*u*

B) = 0.5-0.7*u*

C) = 0.7-0.9*u*

D) = 0.9-1.1*u*

E) = 1.1-1.3*u*

Vertical lines show the average duty factor of the trials. Black = average, red and blue are upper and lower confidence intervals. Y axis is recorded electrical signal after amplification, filtering and rectification.

Figure S2 ILFB average EMG signals across different speeds for emu babies and juveniles. A)-D) babies, E) juveniles. A) = 0.7-0.9*u*, B) = 0.9-1.1*u*, C) and E) = 1.1-1.3*u*, D) = 1.3-1.5*u*.Vertical lines show the average duty factor of the trials. Black = average, red and blue are upper and lower confidence intervals. Y axis is recorded electrical signal after amplification, filtering and rectification but due to different amplification should not be compared between the different age groups.